PHYSICAL REVIEW A VOLUME 35, NUMBER 1 JANUARY 1, 1987

Analysis of the oscillating-cup viscometer for the measurement of viscoelastic properties

R. N. Kleiman
AT&T Bell Laboratories, Murray Hill, New Jersey 07974-2070
(Received 16 October 1985; revised manuscript received 20 August 1986)

We present calculations for the analysis of torsional oscillator measurements of the mechanical properties of viscoelastic fluids and solids. The usefulness of this measurement technique is analyzed and discussed in detail. A right circular cylinder is chosen as a well-defined geometry for accurate calculations. Exact expressions for calculating the fluid viscosity and elasticity from the oscillator response in this geometry are presented and discussed. We believe this to be the first exact treatment of the problem. Simplified expressions valid for certain special cases are presented for ease of calculation and compared to those previously obtained. The range of operation and optimal oscillator designs for general applications are suggested. Finally, use of this technique for measuring the frequency dependence of viscoelastic properties is also examined.

I. INTRODUCTION

There are several physical systems currently of interest which have long-range order with very large unit cells, for example, the liquid-crystal blue phases,[1] colloidal crystals,[2] and certain microemulsion phases.[3] These weakly bound solids are viscoelastic materials, having the properties of both solids and fluids. Their viscoelastic behavior typically has an interesting dependence upon frequency. The liquid-crystal blue phase I for example, has a low shear modulus[1] (~ 1000 dyn/cm^2) and a moderate viscosity (~ 1 poise). The viscosity η of such materials cannot be measured using standard capillary flow techniques due to the effect of the elasticity on the flow properties. The elasticity G cannot be measured using standard techniques since the material flows on laboratory time scales. Oscillating cup viscometry, however, is well suited for the simultaneous measurement of both η and G of viscoelastic materials. A careful measurement of the viscoelastic properties can give detailed information regarding the phase diagram such as transition temperatures and types of transitions as well as supportive evidence regarding the structure.[1] In this paper we will develop the mathematical techniques required to calculate η and G from a measurement of the viscoelastic properties using an oscillating cup viscometer. This is the first exact treatment of the problem. These techniques have been used successfully to calculate the viscoelastic properties of the blue phases from a measurement[1] of their mechanical properties.

There are two distinct experimental approaches towards the measurement of η and G using oscillating cup viscometry. The first consists of placing the viscoelastic fluid in contact with a stable high-Q oscillator and measuring small changes in the oscillator frequency and amplitude due to the presence of the fluid. The second approach consists of placing the fluid in contact with a nonresonant oscillator and measuring the frequency and amplitude of the fluid resonance in a particular geometry. High-Q techniques are better suited for most measurements due to the higher sensitivity and lower shear rates. We will discuss calculations for the high-Q method in Sec. II, and the resonant fluid method, only briefly, in Sec. III.

The case of a simple Newtonian liquid (which by definition has $G=0$) in contact with a right circular cylinder cup oscillator was first solved by Shvidkovskii,[4] and more extensively by Kestin and Newell and Beckwith and Newell.[5] Using the mathematical techniques outlined in the above papers we have solved the somewhat more complicated problem of a viscoelastic fluid (which depends on both η and G) in contact with a right circular cylinder cup oscillator. In this case the parameter space becomes much larger and its application to experiment becomes much different than for a simple liquid. A right circular cylinder is a convenient well-defined geometry for a torsional cup viscometer, but the techniques developed here are also applicable to other similar geometries (spheres, discs, etc.) such as those studied by Kestin *et al.*[6] for simple liquids.

In addition to the mathematical solution, it is important to examine the usefulness of this technique for the measurement of η and G. We will look at the sensitivity of such a cup viscometer for the measurement of η and G, as well as the ease and speed with which calculations can be made. It is also very useful to know the optimal cup design for a given application, where the range of η and G is known approximately. This paper is intended as a guide for those interested in using the powerful technique of oscillating cup viscometry for the measurement of viscoelastic parameters.

II. THE HIGH-Q METHOD

A. Experimental technique

In Fig. 1 we show a picture of a high-Q torsional oscillator configured as an oscillating cup viscometer. This oscillator is composed of a silver right cylindrical cup, a thin torsion member and electrode plate fabricated from single crystal silicon, and a brass base. This oscillator has an empty cell $Q_0 \approx 10\,000$, and a frequency $\omega_0 \approx 128$ Hz. The frequency and amplitude of the oscillator on reso-

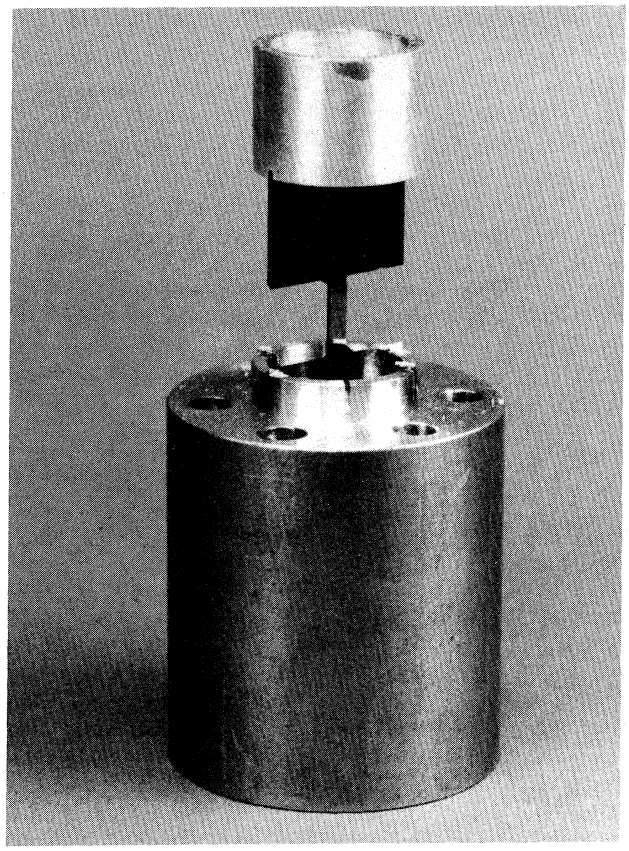

FIG. 1. High-Q torsional oscillator configured as an oscillating cup viscometer. Viscoelastic parameters of a sample can be deduced by measuring the resonant frequency and amplitude of the oscillator when empty and in the presence of the sample. For this oscillator $Q_0 \approx 10\,000$ and $\omega_0 = 128$ Hz.

nance are measured using standard techniques. They can be measured to a high degree of accuracy. The temperature dependence of these quantities is measured both with and without a sample in the cup. From the changes in frequency and amplitude due to the presence of the sample its viscoelastic parameters can be deduced as a function of temperature. The details of constructing and operating high-Q torsional oscillators is discussed in detail in Ref. 7.

There are two common ways of implementing high-Q techniques. In the first, the amplitude and frequency of forced oscillations on resonance are measured. In the second, the frequency and decay time of free oscillations are measured. The first method is preferable because the operating electronics can be configured so that the oscillator is the frequency determining element of a phase-locked loop. The resulting resonant frequencies and amplitudes are very stable and can be easily monitored as a function of some external parameter (the temperature T for example) in an automated fashion. In the free-oscillation case, there can be errors due to the transients associated with starting the free oscillations that are not present in the forced case. In either case, when the fluid is placed in contact with the torsional oscillator there are small changes in the frequency and the Q with respect to the empty cell values. The solutions for Q and ω as functions of η and G are very similar for the above two cases but differ by terms proportional to $(I'/I)^2$ and smaller (where I' and I are the moments of inertia of the fluid and of the oscillator). In the limit where $I'/I \ll 1$, i.e., when the fluid motion is a small perturbation on the oscillator motion (to be discussed in Sec. II F) the solutions become identical. Since we find the forced oscillation case to be experimentally and theoretically preferable, and the differences between the two to be slight, we will confine a discussion of the free-oscillation case to an Appendix.

The frequency of oscillation (ω_0) is fixed and is typically in the range of 1 Hz to 10 kHz. The empty cell Q (Q_0) is typically in the range of 10^4 to 10^6. It is important to have Q_0 high in order to reduce the corrections to the Q, in order to minimize phase errors and for the possibility of studying systems with small damping. It is also helpful to have $d\omega_0/dT$ and dQ_0/dT as small as possible to minimize errors associated with background corrections.

B. Theoretical analysis

(1) For a viscous liquid in contact with an oscillating cup, a boundary layer $\delta \equiv [\eta/(\omega\rho)]^{1/2}$ which we call the viscous penetration depth, is coupled to the oscillator motion. It is easy to show that when $\delta \ll R$ and $\delta \ll H$,

$$S_\omega = S_Q = \frac{I'}{2I}\frac{\delta}{\sqrt{2}H}\left[1+\frac{4H}{R}\right] \tag{1}$$

where

$$S_\omega \equiv \frac{-(\omega-\omega_0)}{\omega_0} \equiv \frac{-\Delta\omega}{\omega_0} ,$$

$$S_Q \equiv \frac{1}{2Q} - \frac{1}{2Q_0} \equiv \Delta - \Delta_0 ,$$

and where we have defined H as the fluid height; R, the fluid radius; ρ, the fluid density; $I' = \frac{1}{2}\rho\pi HR^4$, the fluid moment of inertia; I, the oscillator moment of inertia; $\Delta_0 \equiv 1/2Q_0$, the empty cell decrement; $\Delta \equiv 1/2Q$, the full cell decrement; ω_0, the empty cell oscillator frequency; and ω as the full cell oscillator frequency. The quantities S_ω and S_Q are the dimensionless inertial and dissipative oscillator response, and correspond to the measured frequency and amplitude of oscillation. Mason first showed[8] by substituting a complex viscosity $\eta^* = \eta_r - i\eta_i$ (where $\eta_i = G/\omega$) in place of η that

$$\eta_i = \frac{G}{\omega} = k(S_Q^2 - S_\omega^2) ,$$
$$\eta_r = 2kS_QS_\omega , \tag{2}$$

where

$$k \equiv \omega\rho\left[\frac{2I}{I'}\frac{R}{(4+R/H)}\right]^2 .$$

It is clear that Eq. (2) is the lowest-order solution, but due to the method of derivation it is unclear over what range of parameters it gives meaningful results.

(2) In order to solve the problem of the oscillator

motion for all values of η and G regardless of cup size we must solve the full differential equation. Kestin and Newell and Beckwith and Newell[5] derive the solution to the oscillator motion for the case of free oscillations of a cup oscillator in contact with a simple fluid. They use Laplace transform techniques to solve the differential equation of motion. To describe the technique briefly, we begin with the differential equation of motion of the oscillator including the torque of the fluid on the oscillator. The torque is found using the Navier-Stokes equations, neglecting nonlinear terms as well as surface tension. (All results are correct for the zero amplitude limit, so it is important to work at low shear rates to take advantage of the accuracy of the solution.) Using Laplace transforms, the equation of motion is reduced to a dimensionless partial differential equation which is solved subject to the boundary conditions of a right circular cylinder. The inverse Laplace transform gives the oscillator motion.

We follow the general procedure outlined above with two significant modifications. The first is to add a forcing function, $F_0\sin\omega t$, to the original differential equation in order to also find the steady-state solution. The second is to change the differential equation describing the fluid motion to include its elasticity, G. This becomes

$$\ddot{\Omega}=\frac{\eta}{\rho}\nabla^2\dot{\Omega}+\frac{G}{\rho}\nabla^2\Omega\ , \tag{3}$$

where Ω is the angular velocity and ∇^2 is the Laplacian for polar-cylindrical coordinates. (See, for example, Ref. 2.) Here G and η are the frequency independent parameters to which a viscoelastic model can then be applied. The application of viscoelastic models will be discussed in more detail in Sec. IV.

The solution is composed of three parts: a steady-state solution, a free-oscillation solution (see Appendix), and a sum of infinitely many transients. For the steady-state solution, the latter two can be ignored and we find the oscillator amplitude $\alpha(t)$ is given by

$$\frac{\alpha(t)}{\alpha_0}=\frac{\sin(\omega t+\phi)}{\left\{\left[1-\left[\frac{\omega}{\omega_0}\right]^2+D_r\left[i\frac{\omega}{\omega_0}\right]\right]^2+\left[2\frac{\omega}{\omega_0}\Delta_0+D_i\left[i\frac{\omega}{\omega_0}\right]\right]^2\right\}^{1/2}}\ , \tag{4a}$$

$$\tan\phi=\frac{-\left[\frac{2\omega}{\omega_0}\Delta_0+D_i\left[i\frac{\omega}{\omega_0}\right]\right]}{1-\left[\frac{\omega}{\omega_0}\right]^2+D_r\left[i\frac{\omega}{\omega_0}\right]}\ , \tag{4b}$$

where

$$\alpha_0\equiv\frac{F_0}{I\omega_0^2}\ .$$

In these expressions, D_r and D_i are the real and imaginary parts of $D(s)$, and s is the complex Laplace transform variable, whose value is $s=i\omega/\omega_0$ for the steady-state solution. The function $D(s)$ depends upon the experimental variables η and G, and the constants H, R, I, ω_0, and ρ.

The function $D(s)$ is related to the Laplace transform of the fluid torque $\bar{M}(s)$ by the relation $D(s)=s\bar{M}(s)I\omega_0^2[s\bar{\alpha}(s)-\alpha_0]$. The mathematical problem consists of solving the dimensionless partial differential equation, which describes the fluid motion, subject to the boundary conditions of the given geometry giving $D(s)$ directly. Kestin and Newell[5] present five different expressions for $D(s)$, using different expansion functions. All are mathematically equivalent, but vary in their ease of use, ease of understanding, and convergence for various values of the parameters. We will discuss two of these in Secs. III and IV. The function $D(s)$ for a viscoelastic liquid can be expressed in terms of the function $D(s)$ found in Ref. 5 for a simple liquid by making the substitution

$$\eta\rightarrow\eta_r+\frac{1}{s}\eta_i\ , \tag{5}$$

where η_r and η_i are the real and imaginary viscosities, and defining

$$\eta_i\equiv\frac{G}{\omega_0}\ . \tag{6}$$

In an experiment, the physically measured quantities are typically the resonant amplitude α and frequency ω. In order to find the constants Δ_0 and ω_0 an empty cell run must be taken. The solutions are then expressed as differences between the measured quantities with the oscillator full and empty: $(\alpha_0/2\alpha)_f-\Delta_0$ and $(\omega_f-\omega_0)/\omega_0$ as in Eq. (1). We have sometimes used (ω,α) to abbreviate the set of measured quantities.

In the absence of any fluid $D_r=D_i=0$, and α/α_0 reduces to the familiar forced damped simple harmonic oscillator solution. The resonant amplitude α/α_0 is a maximum when

$$\omega_e^2=\omega_0^2(1-2\Delta_0^2)\ . \tag{7a}$$

Its value at maximum is

$$\left[\frac{\alpha_0}{2\alpha}\right]_e=\Delta_0(1-\Delta_0^2)^{1/2}\ . \tag{7b}$$

The constants ω_0 and Δ_0 arise naturally in the equations which follow, but ω_e and $(\alpha_0/2\alpha)_e$ are the quantities which would be measured in an empty cell background run. For the remainder of this section ω_0 and Δ_0 will be

used, but the substitutions of Eq. (7) must be made for a precise data analysis.

In the presence of the fluid we can calculate the frequency ω_f, at which the maximum in α/α_0 occurs, by differentiating Eq. (4a) with respect to ω. This gives

$$1-\left[\frac{\omega_f}{\omega_0}\right]^2+D_r\left[i\frac{\omega_f}{\omega_0}\right] = \frac{\left[2\Delta_0+\frac{\omega_0}{\omega_f}D_i\left[i\frac{\omega_f}{\omega_0}\right]\right]\left[\Delta_0+\frac{1}{2}D_i'\left[i\frac{\omega_f}{\omega_0}\right]\right]}{\left[1-\frac{\omega_0}{2\omega_f}D_r'\left[i\frac{\omega_f}{\omega_0}\right]\right]}, \tag{8a}$$

where

$$D_r'\left[i\frac{\omega_f}{\omega_0}\right]=\frac{d}{d(\omega/\omega_0)}\left[D_r\left[i\frac{\omega}{\omega_0}\right]\right]\Bigg|_{\omega=\omega_f}$$

and

$$D_i'\left[i\frac{\omega_f}{\omega_0}\right]=\frac{d}{d(\omega/\omega_0)}\left[D_i\left[i\frac{\omega}{\omega_0}\right]\right]\Bigg|_{\omega=\omega_f}.$$

At the maximum we can show that

$$\frac{\alpha_0}{2\alpha}=\left[\tfrac{1}{2}D_i\left[i\frac{\omega_f}{\omega_0}\right]+\frac{\omega_f}{\omega_0}\Delta_0\right] \times\left[1+\left[\frac{\Delta_0+\frac{1}{2}D_i'\left[i\frac{\omega_f}{\omega_0}\right]}{\frac{\omega_f}{\omega_0}-\frac{1}{2}D_r'\left[i\frac{\omega_f}{\omega_0}\right]}\right]\right]^{1/2} \tag{8b}$$

and

$$\tan\phi=-\frac{\left[\frac{\omega_f}{\omega_0}-\frac{1}{2}D_r'\left[i\frac{\omega_f}{\omega_0}\right]\right]}{\left[\Delta_0+\frac{1}{2}D_i'\left[i\frac{\omega_f}{\omega_0}\right]\right]}. \tag{8c}$$

When D_i and D_r are small these reduce to

$$\frac{\Delta\omega}{\omega_0}=\frac{\omega_f-\omega_0}{\omega_0}=\tfrac{1}{2}D_r\left[i\frac{\omega_f}{\omega_0}\right], \tag{9a}$$

$$\frac{\alpha_0}{2\alpha}-\Delta_0=\tfrac{1}{2}D_i\left[i\frac{\omega_f}{\omega_0}\right], \tag{9b}$$

and

$$\tan\phi=-\Delta_0^{-1}. \tag{9c}$$

The phase ϕ between the forcing function and the oscillator is very close to 90° as long as Δ_0 is small. We can also relate the resonant amplitude α to the Q of the resonance in the usual way:

$$\frac{\alpha_0}{2\alpha}\approx\Delta\equiv\frac{1}{2Q}, \tag{10}$$

but since α is the measured quantity and not the Q, we will only calculate $\alpha_0/2\alpha$.

The resonant frequency and amplitude ω_f and $\alpha_0/2\alpha$ can be found exactly for all values of D_i and D_r using Eqs. (8a) and (8b). Unfortunately, Eq. (8a) is a transcendental equation for ω_f. It can be solved asymptotically to high accuracy in a few iterations by the following procedure. The functions D_r, D_i, D_r', and D_i' are all insensitive to small changes in ω_f, so an initial guess of $\omega_f=\omega_0$ is a very good one. Using this value for ω_f we can calculate a new ω_f' using Eq. (8a) for $1-(\omega_f'/\omega_0)^2$. This iteration procedure converges rapidly since the original guess is so close to the final converged value.

(3) The simplest equation for $D(s)$ is one which contains no complicated functional forms:

$$D(s)=\frac{I'}{I}s^2\left[1-\frac{64}{\pi^2}s\sum_{j=1}^{\infty}\sum_{m=0}^{\infty}\frac{1}{\mu_j^2(2m+1)^2(s+s_{jm})}\right] \tag{11}$$

with

$$s_{jm}\equiv\frac{\eta}{\lambda_{jm}^2\rho\omega_0},$$

$$\lambda_{jm}\equiv\left[\left[\frac{\mu_j}{R}\right]^2+\left[\frac{(2m+1)\pi}{H}\right]^2\right]^{-1/2},$$

where the μ_j's are the zeros of the first-order Bessel function of the first kind J_1. (See Ref. 9 for a power series expression to calculate the μ_j's.) In a sense this is the "true" solution, since it was derived using a normal mode expansion where λ_{jm} is the normal mode wavelength. This expression for $D(s)$ is the simplest for analytical work but converges slowly in certain limits due to the double summation. In addition, the errors due to truncating the double summation are hard to assess. This is particularly problematic in the low to medium viscous penetration depth limit where the technique will prove to be most useful.

To find the solution for a viscoelastic fluid using Eq. (11) we make the substitution of Eq. (5), let $s=i\omega/\omega_0$, and separate real and imaginary parts and find

$$D_r\left[i\frac{\omega}{\omega_0}\right]=\frac{-I'}{I}\left[\frac{\omega^2}{\omega_0^2}-\frac{64}{\pi^2}\frac{\omega^4}{\omega_0^4}\times\sum_{j,m}\frac{a}{\mu_j^2(2m+1)^2(s_{jmr}^2+a^2\omega^2/\omega_0^2)}\right], \tag{12a}$$

$$D_i\left[i\frac{\omega}{\omega_0}\right]=\frac{I'}{I}\left[\frac{64}{\pi^2}\frac{\omega^3}{\omega_0^3}\sum_{j,m}\frac{s_{jmr}}{\mu_j^2(2m+1)^2(s_{jmr}^2+a^2\omega^2/\omega_0^2)}\right], \tag{12b}$$

where

$$a=1-\frac{\omega_0^2}{\omega^2}s_{jmi} ,$$

$$s_{jmr}\equiv\frac{\eta_r}{\lambda_{jm}^2\rho\omega_0} ,$$

and

$$s_{jmi}\equiv\frac{\eta_i}{\lambda_{jm}^2\rho\omega_0}\equiv\frac{G}{\lambda_{jm}^2\rho\omega_0^2} .$$

Another disadvantage of this solution is that a leading term expansion does not readily reduce to the low viscous penetration depth solution.

The fluid resonances are apparent due to the nature of the expansion. It is easy to show that for low viscosities, there are fluid resonances when

$$\lambda=\frac{1}{\omega}\left[\frac{G}{\rho}\right]^{1/2}\approx\lambda_{jm} , \tag{13}$$

where λ is the wavelength of the transverse waves traveling through the fluid. These correspond to the normal modes of a solid in a cup geometry. Thus the fluid motion can be thought of as a superposition of infinitely many underdamped or overdamped modes of different wavelengths. It must be kept clear that the oscillator motion is always strongly underdamped, as required by the measurement technique, but the fluid may be underdamped or overdamped. When the fluid is on resonance the system is analogous to a coupled harmonic oscillator, but it is the oscillator's frequency and amplitude that are monitored, not those of the fluid. In Sec. II C we will discuss the region of $(\delta/R,\lambda/R)$ space in which these resonances occur, and in Sec. III we will discuss the fluid resonances themselves.

(4) It is straightforward to show that Eq. (11) can be simplified by recognizing the identity

$$\frac{\tanh(x)}{x}=8\sum_m\frac{1}{(2m+1)^2\pi^2+4x^2} . \tag{14}$$

Use of Eq. (14) significantly reduces the calculation time required, due to the need to sum over only one variable. This comes at the expense of a moderate increase in calculational complexity, but still only requires the evaluation of the sine, cosine, and exponential functions. We find that

$$D(s)=\frac{I'}{I}s^2\left[1-8s\sum_j\frac{1}{\mu_j^2 s_\mu^2}\left[1-\frac{\tanh(x)}{x}\right]\right] , \tag{15}$$

where

$$s_\mu^2\equiv\frac{\eta\mu_j^2}{\rho\omega_0 R^2}+s$$

and

$$x\equiv s_\mu H\left[\frac{\omega_0\rho}{\eta}\right]^{1/2} .$$

After substituting $\eta\rightarrow\eta_r+\eta_i/s$, letting $s=i\omega/\omega_0$, and separating real and imaginary parts we find that

$$D_r\left[i\frac{\omega}{\omega_0}\right]=\frac{-I'}{I}\frac{\omega^2}{\omega_0^2}\left[1+\frac{8\omega^2}{\omega_0^2}\sum_j\frac{e[1-Q_r(a,b)]-fQ_i(a,b)}{\mu_j^2(e^2+f^2)}\right] , \tag{16a}$$

$$D_i\left[i\frac{\omega}{\omega_0}\right]=\frac{I'}{I}\frac{8\omega^4}{\omega_0^4}\left[\sum_j\frac{eQ_i(a,b)+f[1-Q_r(a,b)]}{\mu_j^2(e^2+f^2)}\right] , \tag{16b}$$

where

$$e\equiv k\eta_i-\left[\frac{\omega}{\omega_0}\right]^2 ,$$

$$f\equiv k\frac{\omega}{\omega_0}\eta_r ,$$

$$k\equiv\frac{\mu_j^2}{\rho\omega_0 R^2} ,$$

and

$$Q(a+ib)\equiv\frac{\tanh(a+ib)}{a+ib}=Q_r(a,b)+iQ_i(a,b) .$$

It can be shown that

$$Q_r(a,b)=\frac{a\sinh(2a)+b\sin(2b)}{(a^2+b^2)[\cosh(2a)+\cos(2b)]} ,$$

$$Q_i(a,b)=\frac{a\sin(2b)-b\sinh(2a)}{(a^2+b^2)[\cosh(2a)+\cos(2b)]} ,$$

where

$$a\equiv(1/\sqrt{2})[c+(c^2+d^2)^{1/2}]^{1/2} ,$$

$$b\equiv(1/\sqrt{2})[-c+(c^2+d^2)^{1/2}]^{1/2} ,$$

and we have defined

$$c\equiv H^2\left[\frac{\mu_j^2}{R^2}-\frac{\rho\omega^2\eta_i}{\omega_0[\eta_i^2+(\eta_r\omega/\omega_0)^2]}\right]$$

and

$$d\equiv\frac{H^2\rho\omega^3\eta_r}{\omega_0^2[\eta_i^2+(\eta_r\omega/\omega_0)^2]} .$$

Equations (16a) and (16b) are the best means of calculating $\Delta\omega/\omega_0$ and $\alpha_0/2\alpha$ when speed and accuracy are required. They still converge slowly for very low values of δ/R and λ/R but are ideal for the working region to be described in Sec. II E. Equations (16a) and (16b) provide an exact solution for the steady-state response of a torsional oscillator in contact with a viscoelastic fluid, for all values of η and G, and for any cup size. They are exact to all orders of I'/I as long as the iteration procedure (8) of Sec. II B is followed. It must be emphasized that Eq. (16) is an exact solution: no calibration constants are required and all edge corrections are contained within the solutions.

In Sec. II C we will discuss the behavior of these functions throughout parameter space. In Secs. II D and II E we will discuss errors inherent in the technique which impose limitations on the range of η and G over which the technique can be successfully used. In Secs. II F, II G, and II H we will discuss errors associated with simplified calculation of the functions; such errors can be circumvented completely by a more time-consuming exact calculation.

C. Map of oscillator response to a viscoelastic fluid

To give the reader a feeling for the nature of the functions $(\Delta\omega/\omega_0)(G,\eta)$ and $(\alpha_0/2\alpha)(G,\eta)$ we show in Figs. 2(a) and 2(b) contour plots of these functions over a wide range of G and η. Each line represents the locus of points that have the same value of the function. If we choose the dimensionless plotting coordinates δ/R and λ/R instead of η and G, then the contour plots give both a good quantitative as well as qualitative picture of the functions. Thus with the proper rescaling of parameters the contour plots in all figures can be used as master curves to avoid tedious recalculations. The cup size, oscillator frequency, and fluid density are scaling parameters for δ and λ. The magnitude of the functions are proportional to I'/I as long as I'/I is reasonably small. The functional form of the equations is only weakly dependent on the cup shape R/H, outside of the resonant region.

Since there is a unique mapping of $(G,\eta)\rightarrow(\lambda,\delta)$ all values of G and η can be rescaled according to the following equations:

$$\frac{\delta}{R}=\frac{1}{\omega_0 R}\left[\frac{\eta\omega_0}{\rho}\right]^{1/2}, \tag{17a}$$

$$\frac{\lambda}{R}=\frac{1}{\omega_0 R}\left[\frac{G}{\rho}\right]^{1/2}, \tag{17b}$$

to find the location of a given experimental arrangement in phase space. The parameter δ/R is the dimensionless viscous penetration depth and is the characteristic length associated with the liquidlike properties of the viscoelastic material. Similarly, λ/R is the dimensionless wavelength and is the characteristic length associated with solidlike properties of the material.

For simplicity, the aspect ratio of the cup R/H is chosen to be $R/H=(2\mu_1/\pi)\approx 2.44$. In a sense this is the midway point between $R/H\gg 1$ and $R/H\ll 1$. For values of R/H around unity the functions are only weakly dependent upon this ratio. Since the smaller length dominates, one should calculate and plot $\delta/R,\lambda/R$ if $R/H<2.44$, and if $R/H>2.44$ one should use $\delta/2.44H$ and $\lambda/2.44H$ as plotting parameters to minimize any dependence on R/H.

It is apparent from Eqs. (16a) and (16b) that the height of these curves is proportional to I'/I, and thus can easily be rescaled given a new value of I'/I. For the value of R/H chosen above, it is possible to show that the point of maximum damping in the $G\rightarrow 0$ limit occurs when $\delta/R\approx 0.15$. At this point $Q_{\min}\approx 3I/I'$; thus we must make I'/I reasonably small to prevent the Q from dropping to too low a value. The Q is kept high for many reasons: high stability, low bandwidth for coupling in mechanical noise, and low I'/I corrections (as will be discussed in Sec. II F). We have chosen $I'/I\approx\frac{1}{32}$, so that $Q_{\min}=100$, a reasonable lower limit. The constant Q_0 is assumed to be high, so we have set $\Delta_0\equiv 1/2Q_0=0$.

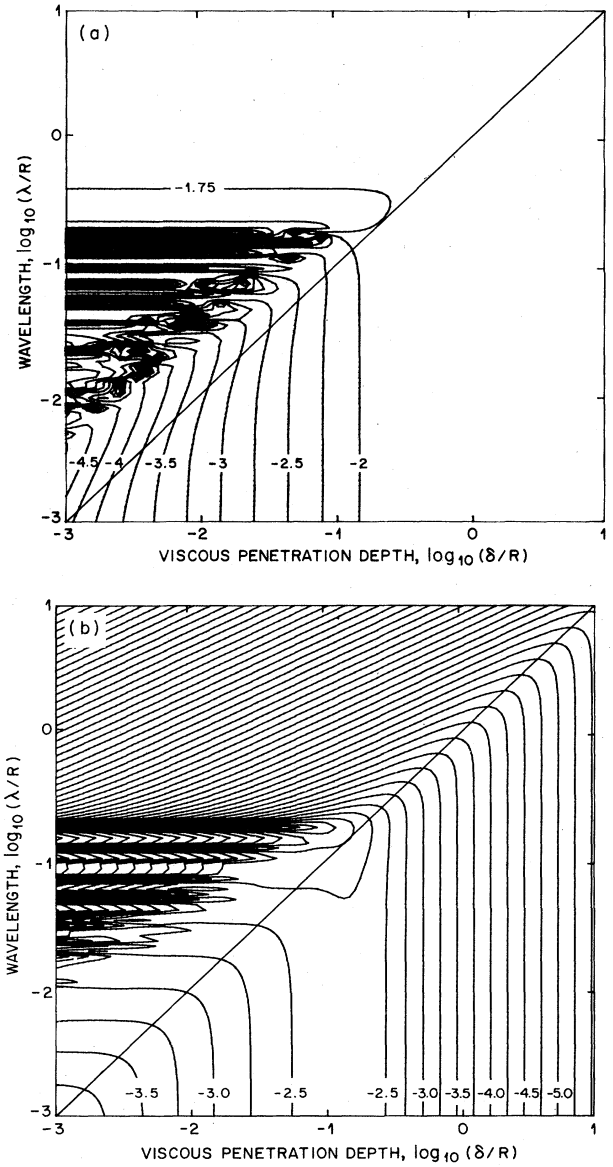

FIG. 2. Contour plots of the real and imaginary parts of the dimensionless response of an oscillator to a viscoelastic fluid throughout $(\delta/R,\lambda/R)$ space. The parameters δ/R and λ/R are the dimensionless viscous penetration depth and wavelength corresponding to the liquidlike and solidlike length scales compared to the cup size. (a) Dimensionless inertial response $\log_{10}(|\Delta\omega/\omega_0|)$ corresponding to a small change in the oscillator resonant frequency. (b) Dimensionless dissipative response $\log_{10}(\alpha_0/2\alpha)$ corresponding to the oscillator resonant amplitude. Dark areas correspond to regions with densely spaced fluid resonances. Absolute height of the curves is proportional to I'/I. We have set $R/H=2.44$, $I'/I=0.0312$, $1/2Q_0=0$. These same constants are used for the remainder of the figures.

It is fairly easy to understand the nature of the functions $\Delta\omega/\omega_0$ and $\alpha_0/2\alpha$. When λ/R is small (the $G\to 0$ limit), the functions behave as we expect for a viscous liquid. When $\delta/R \ll 1$ both $\Delta\omega/\omega_0$ and $\alpha_0/2\alpha$ vary smoothly in the same way with δ/R. When $\delta/R \approx 1$ there is a maximum in the dissipation, and the slope of $\Delta\omega/\omega_0$ versus δ/R is largest. When $\delta/R \gg 1$ then both $\Delta\omega/\omega_0$ and $\alpha_0/2\alpha$ saturate.

On the other hand, when $\lambda/\delta < 1$ all resonant modes in the fluid are overdamped because the acoustic wavelength λ is shorter than δ the decay length associated with the damping of acoustic waves. Whereas if $\lambda > \delta$ the modes are underdamped. The line $\lambda=\delta$ is shown for comparison. The principal resonant mode (TA10) occurs when $\lambda \approx R$ ($\lambda=0.185R$), with the higher frequency modes at shorter wavelengths. When $\lambda/R \gg 1$ then both $\Delta\omega/\omega_0$ and $\alpha_0/2\alpha$ are saturated. This leaves one octant of phase space strongly resonant.

D. Oscillator sensitivity for different viscoelastic parameters

It is natural to ask with what accuracy we can measure G and η in various regions of $(\lambda/R,\delta/R)$ space. This would tell us something about the useful regions of $(\lambda/R,\delta/R)$ space for measurement purposes and the accuracy with which we need to measure the frequency and amplitude. It is easy to show that

$$E_{G,\eta}(\lambda/R,\delta/R)=\left[\left[\frac{\Delta G}{G}\right]^2+\left[\frac{\Delta\eta}{\eta}\right]^2\right]^{1/2}$$

$$=F(\lambda/R,\delta/R)E_{\omega,\alpha}\ , \qquad (18)$$

where

$$F(\lambda/R,\delta/R)=\left[\frac{1}{G^2}+\frac{1}{(\eta\omega_0)^2}\right]^{1/2}(a^2+b^2)^{-1/2}\ ,$$

$$a\equiv\left|\frac{\partial\left[\frac{\Delta\omega}{\omega_0}\right]}{\partial G}\right|=\left|\frac{\partial\left[\frac{\alpha_0}{2\alpha}\right]}{\partial\eta\omega_0}\right|\ ,$$

and

$$b\equiv\left|\frac{\partial\left[\frac{\Delta\omega}{\omega_0}\right]}{\partial\eta\omega_0}\right|=\left|\frac{\partial\left[\frac{\alpha_0}{2\alpha}\right]}{\partial G}\right|\ .$$

Here, $E_{\omega,\alpha}$ is the amount of noise associated with the measurement of frequency $(\Delta\omega/\omega_0)$ or amplitude $[(1/2Q)(\Delta\alpha/\alpha)]$ expressed in fractional units, and $E_{G,\eta}$ is the error associated with G and η. Equation (18) treats the noise from frequency and amplitude sources identically, but this is justified because for experimental reasons they are usually similar. Since we are concerned with knowing *both* G and η, Eq. (18) emphasizes the parameter known most poorly. In the oscillating cup technique G is often known more poorly. The apparent error in η at a particular point in $(\lambda/R,\delta/R)$ space may be overestimated, but in doing so we clearly know the accuracy with which we know both parameters. Figure 3 shows a contour plot of $\log_{10}[F(\lambda/R,\delta/R)]$. (Only lines for which $F<4$ are shown.) As an example, if we can measure the frequency and amplitude to one part in 10^6, then along the outer contour line whose height is 4, we can measure both G and η to one part in 10^2. Thus F is essentially the error transfer function. It tells us the amount of error transferred to the quantities of interest, η and G, due to random or systematic errors in the measured ω and α. Random noise in ω and α will limit our ability to resolve features in G and η. Systematic errors in ω and α, due to offset errors for example, will cause shifts in the determined values of η and G, but may not obscure features in them.

The height of the level curves is proportional to $(I'/I)^{-1}$. Different values of I'/I must be rescaled accordingly. The lower $Q_{\min}$ is, the higher the resolution, at a fixed noise level[10] for reasonable values of $Q_{\min}$. There clearly is a tradeoff in choosing $Q_{\min}$; it must be kept high for the reasons previously outlined in Sec. II C, but low enough to have sufficient resolution as well as insensitivity to systematic errors. Since we have chosen a reasonable lower limit for $Q_{\min}$ ($Q_{\min}=100$), Fig. 3 appears to represent a best case. For higher values of $Q_{\min}$, the region in which $F<4$ will shrink. However, when $\delta \ll R$ and $\lambda \ll R$ the Q may never fall as low as $Q_{\min}$, and it is possible to reduce $Q_{\min}$ accordingly. By reducing $Q_{\min}$ the region of high resolution can be extended somewhat, but the range of viscoelastic parameters that can be

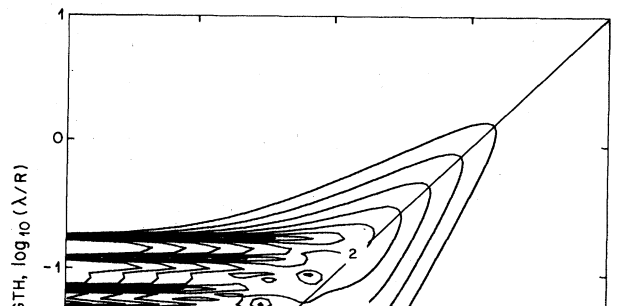

FIG. 3. Contour plot of the total fractional error $E_{G,\eta}$ in both G and η associated with fractional errors $E_{\omega,\alpha}$ due to noise in ω and α. $E_{G,\eta}\approx(\Delta\omega/\omega_0)E_{\omega,\alpha}\approx(1/2Q)(\Delta\alpha/\alpha)E_{\omega,\alpha}=FE_{\omega,\alpha}$ where $\log_{10}(F)$ is the value labeled on the curves. Height of the curves is proportional to $(I'/I)^{-1}$ and is plotted on a $\log_{10}$ scale. In the center region of the plot, the determination of (G,η) is least sensitive to uncertainties in the measurement of the oscillator response.

measured will be reduced. With care an oscillator can be designed with quite high overall resolution, but this sensitive region is in a rather small region of $(\lambda/R,\delta/R)$ space.

E. Unique conversion

We see from Fig. 3 that the oscillator is very sensitive in the resonant part of $(\lambda/R,\delta/R)$ space. But in order for the oscillating cup technique to be useful for extracting (G,η) from (ω,α) it must be possible to carry out this conversion uniquely. If there are two solutions to (G,η) as a function of (ω,α) near to each other in $(\lambda/R,\delta/R)$ space then there will be an ambiguity as to the correct solution. So clearly it is impossible to operate in regions where multiple solutions exist nearby, such as when the fluid is resonant. Shown in Fig. 4 is the region within which nearest identical solutions are separated by a factor of 4 in η and G, i.e., $[(G_1/G_0)^2+(\eta_1/\eta_0)^2]^{1/2}\leq 4$. This is an arbitrary but useful criterion. If the solutions differ by more than 4, the correct one could probably be chosen on physical grounds, or by continuity. This multiple valued region, as expected, corresponds exclusively to the region where the fluid is resonant.

In much of this region the iteration procedure (8) of Sec. II B also fails. Small changes in ω lead to large changes in D_r and D_i, and so the iteration procedure is unstable. This region must be avoided for the unique conversion of $(\omega,\alpha)\rightarrow(G,\eta)$.

In order to be able to measure η and G using this technique, we must work in the part of Fig. 3 where we have sufficient resolution, and in the part of Fig. 4 where the conversion $(\omega,\alpha)\rightarrow(G,\eta)$ can be carried out uniquely. We refer to this region as the "working region" of the high-Q oscillating cup viscometer. This region is shown with a dotted line in Figs. 5–7.

F. I'/I errors

As alluded to in procedure (8) of Sec. II B Eq. (16) can be simplified considerably under the assumption $I'/I\ll 1$. This is especially warranted since the technique being used is a high-Q technique, and it is desirable to keep I'/I small. In this limit, the solutions for free and forced oscillations become identical (see Appendix). Calculations can be simplified and done more quickly, but first we must assess the errors incurred by making this approximation.

When $I'/I\ll 1$, $\omega_f\approx\omega_0$, so we can rewrite Eqs. (16a) and (16b) as

$$\frac{\Delta\omega}{\omega_0}=\tfrac{1}{2}D_r(i)=\frac{-I'}{2I}\left[1+8\sum_j\frac{e[1-Q_r(a,b)]-fQ_i(a,b)}{\mu_j^2(e^2+f^2)}\right], \tag{19a}$$

$$\frac{\alpha_0}{2\alpha}-\Delta_0=\tfrac{1}{2}D_i(i)=\frac{I'}{2I}\left[8\sum_j\frac{eQ_i(a,b)+f[1-Q_r(a,b)]}{\mu_j^2(e^2+f^2)}\right], \tag{19b}$$

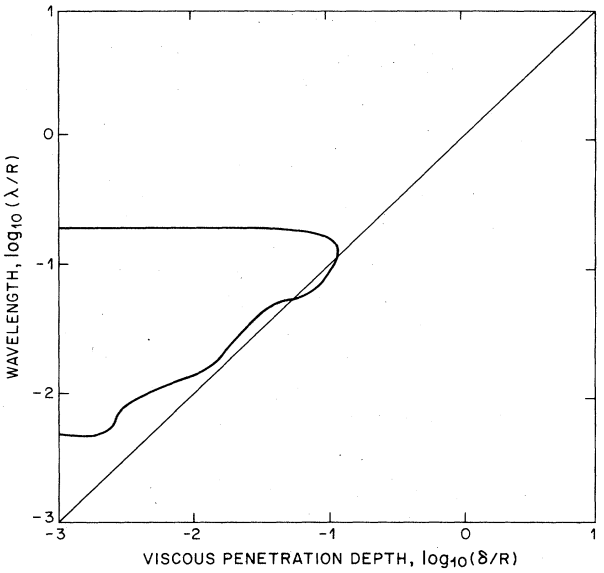

FIG. 4. Region in which identical solutions exist near each other. Within this region the nearest identical solution to $(\omega,\alpha)\rightarrow(G,\eta)$ differs by less then a factor of 4 in one or both of the parameters G and η. For example, if (G_1,η_0) and (G_2,η_0) are nearby solutions to (ω,α), then $0.25<G_1/G_2<4$ within the region shown.

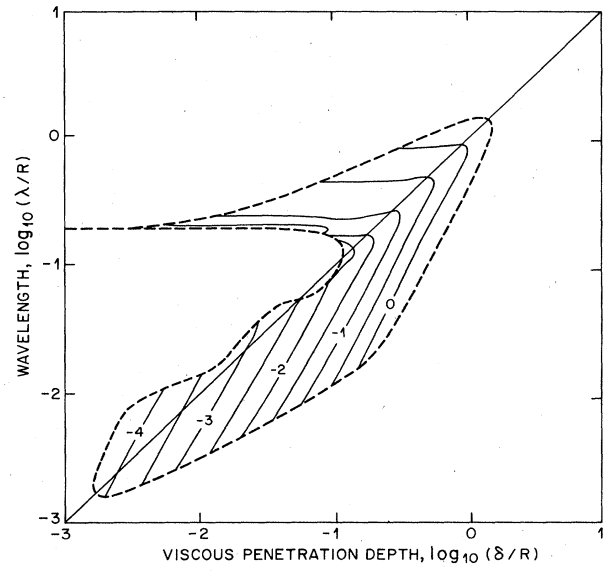

FIG. 5. Contour plot of the total fractional error in both G and η associated with neglecting terms of order $(I'/I)^2$ and smaller. Height of the curves is approximately proportional to I'/I, and is plotted on a $\log_{10}$ scale. Only the region in which the error is less than 100% is shown. Working region of the oscillating cup viscometer is outlined by the dotted line in this and subsequent figures. This region is essentially the intersection of Figs. 3 and 4. Within the working region the oscillating cup viscometer has good resolution and unique solutions for reasonable values of measurement noise and I'/I.

where e and f simplify to

$$e \equiv k\eta_i - 1$$

and

$$f \equiv k\eta_r ,$$

and c and d simplify to

$$c \equiv H^2 \left[\frac{\mu_j^2}{R^2} - \frac{\rho\omega_0\eta_i}{\eta_r^2+\eta_i^2} \right]$$

and

$$d \equiv \frac{H^2\rho\omega_0\eta_r}{\eta_r^2+\eta_i^2} ,$$

with a,b, $Q_r(a,b)$, $Q_i(a,b)$, and k as defined in Sec. II B, procedure (4). [Equation (12) can be similarly simplified.] In doing so Eqs. (19a) and (19b) are no longer transcen-

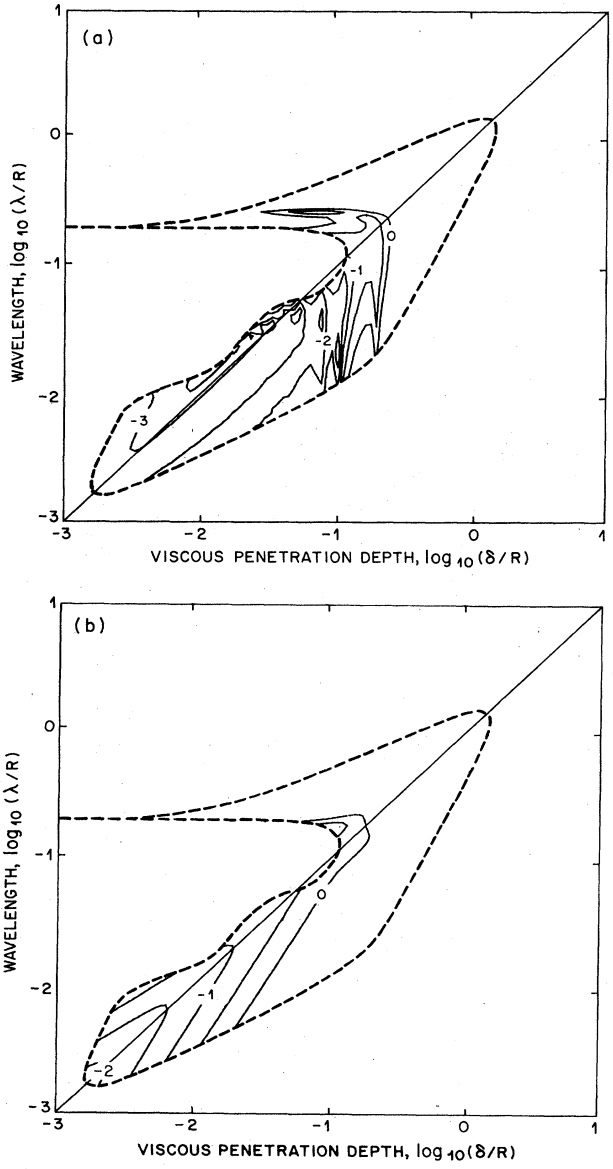

FIG. 6. Contour plots of total fractional error in both G and η associated with using leading terms of a large cup expansion. (a) Four-term expansion and (b) one-term expansion (Mason approximation). Height of the curves is independent of I'/I and is plotted on a $\log_{10}$ scale. Only the region in which the error is less than 100% is shown.

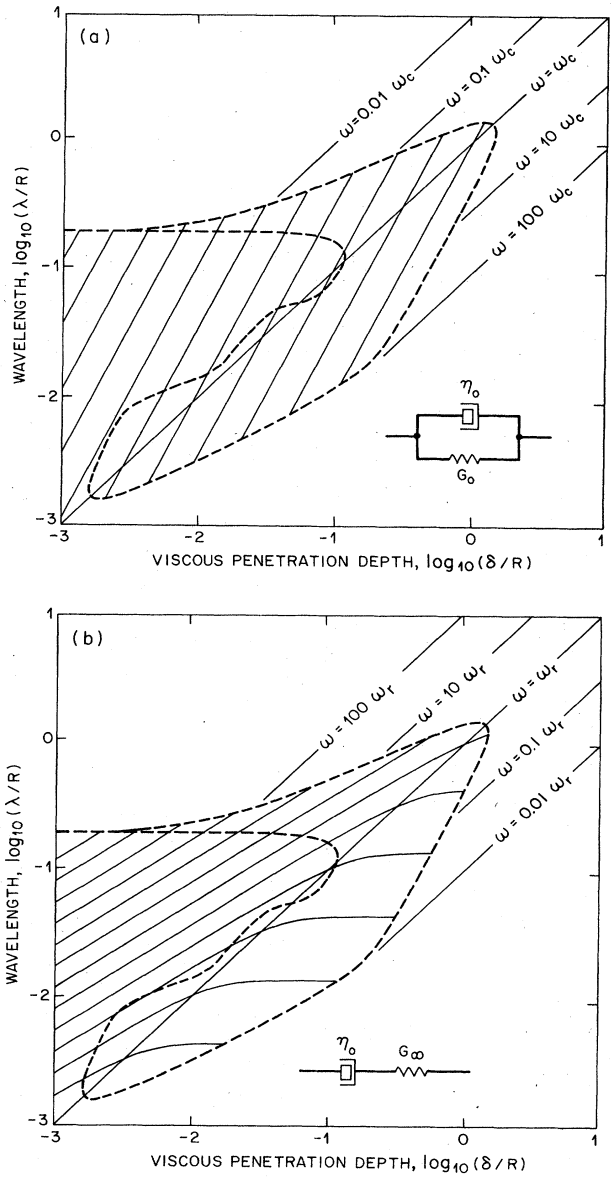

FIG. 7. Lines of constant cup radius R and varying frequency ω within the working region of the oscillating cup viscometer for two simple viscoelastic models. (a) Frequency independent Voigt model ($\omega_c = G_0/\eta_0$). (b) Frequency dependent Maxwell model ($\omega_r = G_\infty/\eta_0$). Corresponding lines of constant ω are also shown. Values of L/R are read from the curves by the value of λ/R or δ/R when lines of constant R intersect the $\lambda/R = \delta/R$ dividing line. Spacing between lines of constant R is 0.5 on a $\log_{10}$ scale.

dental, but become simple one parameter sums with no iteration required. Since we know $\Delta\omega/\omega_0$ and $\alpha_0/2\alpha$ exactly from Eqs. (16a) and (16b) and the iteration procedure (8) of Sec. II B, it is possible to calculate the fractional error $[(\Delta G/G)^2+(\Delta\eta/\eta)^2]^{1/2}$, incurred in G and η in all of $(\lambda/R,\delta/R)$ space due to the omission of higher order terms in I'/I. Thus we can assess the range where this simplication can be used to reduce calculation time. In Fig. 5 is shown a contour plot of $\log_{10}[(\Delta G/G)^2+(\Delta\eta/\eta)^2]^{1/2}$.

From Fig. 5 we can see that for this value of I'/I, the errors incurred due to neglecting higher order terms in I'/I exceed 100% in parts of the working region. In the region where the errors exceed 1%, it is necessary to use the expressions which are exact for all orders of I'/I. The height of these curves is approximately proportional to I'/I, so different values of I'/I can be rescaled accordingly. Since a low value of $Q_{\min}$ is shown, the plots essentially describe a worst case. As I'/I is decreased, the errors will also decrease. However, the sensitive region of Fig. 3 will also shrink. It must be kept in mind that these errors need not be incurred since the iteration scheme (8) of Sec. II B is fast and simple.

G. Large cup expansions

Part of the sensitive range of Fig. 3 includes regions in which $\delta/R<1$ and $\lambda/R<1$. We might expect that a large cup ($\delta/R\ll 1$ and $\lambda/R\ll 1$) expansion would be adequate in that range, and certainly much faster for calculations. An expansion of this type is likely to be valid when $\delta\ll R$, $\lambda\ll R$, but also only when $\lambda<\delta$ since we expect it to be poor at describing resonance phenomena. We start with the large cup expansion[5] for $D(s)$ carried out to four terms:

$$D(s)=\frac{I'}{I}s^2\left\{\frac{\delta}{s^{1/2}R}\left\{4+g\left[1-2\exp\left[\frac{-2s^{1/2}H}{\delta}\right]\right]\right\}-\frac{2\delta^2}{sR^2}\left[3+\frac{8g}{\pi}\right]+\frac{3\delta^3}{2s^{3/2}R^3}(1+6g)+\frac{\delta^4}{2s^2R^4}\left[3-\frac{16g}{\pi}\right]+\cdots\right], \tag{20}$$

where

$$\delta\equiv\left[\frac{\eta}{\rho\omega_0}\right]^{1/2}$$

and

$$g\equiv R/H\ .$$

After substituting $\eta\rightarrow\eta_r+\eta_i/s$, letting $s=i\omega/\omega_0$, and separating real and imaginary parts we find that

$$D_r\left[i\frac{\omega}{\omega_0}\right]=\frac{-I'}{I}\left[\frac{\omega}{\omega_0}\right]^2\left\{\frac{1}{\sqrt{2}f}\{a(4+g)-2ge^{-ca}[a\cos(cb)-b\sin(cb)]\}+\frac{2\eta_i\omega_0}{f^2\omega}\left[3+\frac{8g}{\pi}\right]-\frac{3(b\eta_r+a\eta_i\omega_0/\omega)}{2\sqrt{2}f^3}(1+6g)-\left[\eta_r^2-\left[\frac{\omega_0\eta_i}{\omega}\right]^2\right]\left[3-\frac{16g}{\pi}\right]\right\}, \tag{21a}$$

$$D_i\left[i\frac{\omega}{\omega_0}\right]=\frac{I'}{I}\left[\frac{\omega}{\omega_0}\right]^2\left[\frac{1}{\sqrt{2}f}\{b(4+g)+2ge^{-ca}[b\cos(cb)+a\sin(cb)]\}-\frac{2\eta_r}{f^2}\left[3+\frac{8g}{\pi}\right]+\frac{3(a\eta_r-b\eta_i\omega_0/\omega)}{2\sqrt{2}f^3}(1+6g)-\frac{\eta_i\eta_r\omega_0}{f^4\omega}\left[3-\frac{16g}{\pi}\right]\right], \tag{21b}$$

where

$$a\equiv S_r-S_i\ ,$$

$$b\equiv S_r+S_i\ ,$$

$$S_r\equiv\frac{1}{\sqrt{2}}\left\{\left[\eta_r^2+\left[\frac{\omega_0\eta_i}{\omega}\right]^2\right]^{1/2}+\eta_r\right\}^{1/2},$$

$$S_i=\frac{1}{\sqrt{2}}\left\{\left[\eta_r^2+\left[\frac{\omega_0\eta_i}{\omega}\right]^2\right]^{1/2}-\eta_r\right\}^{1/2},$$

$$f\equiv R(\omega\rho)^{1/2}\ ,$$

$$g\equiv R/H\ ,$$

and

$$c \equiv \frac{\sqrt{2}f}{g[\eta_r^2+(\eta_i\omega_0/\omega)^2]^{1/2}} .$$

If I'/I is large and the higher-order terms cannot be neglected then Eq. (21) must be used together with the iteration procedure (8) of Sec. II B. When $I'/I \ll 1$ we can let $\omega=\omega_0$ and no iteration procedure is required, as was true in the previous section. In this case the series can be inverted; the result is given in the following section. The last term in the first line of each series is the lowest-order term describing interference between the top and bottom of the fluid, and thus the lowest-order resonance term. If we look at the largest term in each series we find approximately that

$$\frac{\Delta\omega}{\omega_0} = \frac{-I'}{2I}\frac{a(4+g)}{\sqrt{2}f}$$

and

$$\Delta-\Delta_0 = \frac{I'}{2I}\frac{b(4+g)}{\sqrt{2}f} .$$

After some rewriting, we recognize these as being identical to Eq. (2), derived by Mason.[8]

It is natural to inquire about the size of the errors incurred in G and η by using Eq. (21) or just Eq. (2) in various parts of $(\lambda/R,\delta/R)$ space. As in Sec. II F we can calculate the fractional error $[(\Delta G/G)^2+(\Delta\eta/\eta)^2]^{1/2}$ exactly since we know $\Delta\omega/\omega_0$ and $\alpha_0/2\alpha$ everywhere from Eqs. (16a) and (16b). Shown in Fig. 6(a) is a contour plot of the fractional errors for the four term expansion of Eq. (21). Shown in Fig. 6(b) is a similar plot for the lowest-order term of the expansion, Eq. (2). The height of these level curves is independent of I'/I as the degree of error is only due to the size of δ/R and λ/R.

Figure 6(a) shows the region in which the four term approximation gives errors less than 100%. This region is within the expected bounds of $\delta \leq R$, $\lambda \leq R$, and $\lambda < \delta$, but we also find that λ/R must be reasonably large. As with the contour plot of Fig. 3, the fractional errors in G grow very large as $G \to 0$. When $\delta < 0.08R$ the four term approximation gives results to better than 1%, and is very useful for fast reasonably accurate calculations. Figure 6(b) shows us that the Mason solution nowhere gives results better than $\approx 1\%$. As expected, its useful range is at lower $\delta/R,\lambda/R$ and with the additional constraints described above. This leaves the Mason solution as only an approximate one, useful for order of magnitude calculations, and fast simple first guesses for iteration procedures (as described in the following section). Equation (21) can be used as a reasonable calculation in the range shown, but outside of this region and for more accurate calculations it is necessary to use the full solution of Eqs. (16a) and (16b).

H. Reversion procedures

(1) Of all the solutions discussed thus far, only the Mason approximation could easily be written as $G(\omega,\alpha)$ and $\eta(\omega,\alpha)$ [see Eq. (2)]. However, Eqs. (8), (19), and (21) all give $\Delta\omega/\omega_0$ and $\alpha_0/2\alpha$ as functions of (G,η). In practice these can easily be inverted by the following reversion scheme, provided that $\Delta\omega/\omega_0$ and $\alpha_0/2\alpha$ are monotonic and we have a reasonable guess for G and η. Let (G',η') be the guessed solution. The parameters $(\Delta\omega/\omega_0)(G,\eta)$ and $(\alpha_0/2\alpha)(G,\eta)$ are the known values of the functions at the unknown (G,η). Then we can write

$$\frac{\Delta\omega}{\omega_0}(G,\eta)-\frac{\Delta\omega}{\omega_0}(G',\eta')=(G-G')\frac{\partial}{\partial G}\frac{\Delta\omega}{\omega_0}(G',\eta')+(\eta-\eta')\frac{\partial}{\partial\eta}\frac{\Delta\omega}{\omega_0}(G',\eta') \tag{22a}$$

and

$$\frac{\alpha_0}{2\alpha}(G,\eta)-\frac{\alpha_0}{2\alpha}(G',\eta')=(G-G')\frac{\partial}{\partial G}\frac{\alpha_0}{2\alpha}(G',\eta')+(\eta-\eta')\frac{\partial}{\partial\eta}\frac{\alpha_0}{2\alpha}(G',\eta') . \tag{22b}$$

The differences $(G-G')$ and $(\eta-\eta')$ can be solved for, giving new and better guesses for G' and η'. The whole process can be iterated quickly to arbitrary accuracy. For this procedure the derivatives can be calculated numerically or calculated analytically and evaluated. The Mason approximation is very convenient to use in the range of Fig. 6(b) as a suitable guess to start the reversion procedure. This reversion procedure will oscillate for $G \approx 0$ unless some care is taken to ensure that $\Delta\omega/\omega_0$ and $\alpha_0/2\alpha$ are continuous through $G=0$.

(2) In some cases it would be convenient to have the inverse polynomial expansion of Eq. (21), expressing G and η as a power series in $\Delta\omega/\omega_0$ and $\alpha_0/2\alpha$. This can be done for all terms in the series with the exception of the exponential term, using reversion of series. We have carried this out for the four terms in Eq. (20), with the result

$$\eta_r = \frac{\rho R^2\omega_0}{2a_1^2}[2F_rF_iC_1+(F_r^2-F_i^2)C_2] , \tag{23a}$$

$$\eta_i = \frac{\rho R^2\omega_0}{2a_1^2}[(F_i^2-F_r^2)C_1+2F_rF_iC_2] , \tag{23b}$$

where

$$C_1 \equiv 1+\frac{a_2}{a_1^2}F_r+\frac{p_1}{4}(F_r^2-F_i^2)+\frac{p_2}{2}F_rF_i ,$$

$$C_2 \equiv \frac{a_2}{a_1^2}F_i+\frac{p_2}{4}(F_i^2-F_r^2)+\frac{p_1}{2}F_rF_i ,$$

the measured quantities are defined as

$$F_r = -\frac{2I}{I'}\frac{\Delta\omega}{\omega_0} ,$$

$$F_i = \frac{2I}{I'}(\Delta - \Delta_0) ,$$

where

$$p_2 = 5a_2a_3 + a_1a_4 - \tfrac{5}{2}a_2^3/a_1 ,$$

$$p_1 = 5a_2^2 - 4a_1a_3 - p_2 ,$$

$$a_1 = \frac{4+g}{\sqrt{2}} ,$$

$$a_2 = 2\left[3 + \frac{8g}{\pi}\right] ,$$

$$a_3 = \frac{3}{2}\frac{1+6g}{\sqrt{2}} ,$$

$$a_4 = \frac{1}{2}\left[3 - \frac{16g}{\pi}\right] ,$$

and

$$g \equiv R/H .$$

This expansion neglects terms of order $(I'/I)^2$ and higher-order terms in I'/I, since it is difficult to include them in the reversion of series. It is required then that $I'/I < (\delta/R)^4$ for all terms in Eq. (23) to be significant. Since I'/I must be reasonably small for stable operation, this condition fails only when λ/R and δ/R are small, so the higher order terms in both δ/R and I'/I are very small and can be neglected in most cases. The higher-order terms can be included by using Eq. (21), the iteration scheme (8) of Sec. II B, and the reversion procedure of Eq. (22).

We recognize the first term in each of Eqs. (23a) and (23b) as being the Mason approximation of Eq. (2). A contour plot of the errors associated with using Eq. (23) looks almost identical to Fig. 6(a) in the working region. The exponential term included in Eq. (21) but neglected in Eq. (23) only improves the approximation near the resonant region, as we would expect, so omitting it has little effect. As seen in Fig. 6(a) the errors associated with using Eq. (23) in the working region are less than 1% when $\delta < 0.08R$. Equation (23) is a very fast direct way to calculate η and G from ω and α when $\delta < 0.08R$ and the I'/I corrections are small.

I. Summary

We have developed an exact method for calculating the fluid elasticity and viscosity (G,η) from the oscillator resonant frequency and amplitude (ω,α) for all values of the parameters. The solution requires the use of Eq. (16), the iteration procedure (8) of Sec. II B, and the reversion procedure of Eq. (22). When $I'/I \ll 1$, Eq. (16) is somewhat simplified and the iteration procedure is not required. When $\delta \ll R$ and $\lambda \ll R$ Eq. (16) is considerably simplified. When $I'/I \ll 1$, $\delta \ll R$, $\lambda \ll R$, and $\lambda < \delta$ Eq. (23) gives the solution directly.

The oscillator must be operated in a region of $(\lambda/R,\delta/R)$ space where there is adequate resolution. It must be operated where G and η can be uniquely determined. The intersection of these two regions is shown by the dotted line in Figs. 5 and 6. For a specific application it is possible to operate outside the working region, but at the cost of a smaller range of operation.

Since we have an exact solution for $(\omega,\alpha) \rightarrow (\eta,G)$ the ultimate limit to the size of the systematic errors is not due to calculation errors, but to the accurate determination of the various constants H, R, ρ, and I. The density ρ may be a function of the external experimental parameters and may have to be measured in a separate experiment, though the determination of (G,η) is largely insensitive to moderate changes in ρ. The surface tension can give rise to an uncertainty in the value of H, and otherwise perturb the surface shape. The significance of this effect has not been assessed.

We can use Figs. 2—6 and the accompanying discussion to aid us in designing an oscillator for a particular application. Given a prior knowledge of G and η Fig. 3 tells us the sensitivity we would have for any value of R and I'/I. Figures 2(a) and 2(b) tell us the magnitude of the quantities we would measure. Figures 5 and 6 suggest regions to operate in, to reduce the time and complexity of data reduction. In order to maintain adequate resolution, δ/R and λ/R cannot be too small nor too large. Furthermore, we must have $\lambda \lesssim \delta$ in order to keep the fluid overdamped. $\lambda \approx 0.1R$ and $\delta \approx 0.2R$ is a reasonable design to aim for. The ratio of moments of inertia I'/I should be kept small enough to keep the Q in an operative range, but large enough for adequate resolution. The value $I'/I \approx 0.01$ is a reasonable tradeoff of these factors. Clearly it may be difficult to maintain all these conditions simultaneously for a viscoelastic fluid whose properties are changing, as a function of temperature, for example. But a knowledge of these guidelines can help optimize cell design.

III. THE RESONANT FLUID METHOD

There are various ways of implementing the resonant fluid method to measure the viscoelastic parameters of a fluid.[2] A standard technique is to place the fluid into a right circular cylinder which oscillates at fixed amplitude. The fluid motion can be monitored at some point in the fluid by a variety of techniques. The frequency of oscillation can be varied, and the consequent amplitude of the fluid motion, as well as its phase with respect to the cup can be monitored.

In order to derive the oscillator response to a viscoelastic fluid in Sec. II B it was necessary to derive the fluid motion throughout the cup. We can show that the fluid angular position α throughout the cup is given by

$$\frac{\alpha(r,h,\omega,t)}{\alpha_F} = -(A_r^2 + A_i^2)^{1/2}\sin(\omega t + \phi) , \tag{24a}$$

$$\tan\phi = \frac{A_i}{A_r} , \tag{24b}$$

where $\alpha_F = F_0/I\omega^2$ is the cup amplitude and is equal to the fluid amplitude as $\omega \rightarrow 0$;

$$A_r = 1 - \frac{8}{\pi}\sum_{j,m} \frac{(s_{jmi}-1)\sin\left[\frac{(2m+1)\pi h}{2H}\right]\frac{R}{r}\frac{J_1(\mu_j r/R)}{J_0(\mu_j)}}{\mu_j(2m+1)[(s_{jmi}-1)^2+s_{jmr}^2]},$$

and

$$A_i = \frac{8}{\pi}\sum_{j,m} \frac{s_{jmr}\sin\left[\frac{(2m+1)\pi h}{2H}\right]\frac{R}{r}\frac{J_1(\mu_j r/R)}{J_0(\mu_j)}}{\mu_j(2m+1)[(s_{jmi}-1)^2+s_{jmr}^2]}.$$

The constants s_{jmi}, s_{jmr}, H, R, and μ_j are all as previously defined (except that ω_0 is no longer the resonant frequency—it is now the oscillator frequency). The variables h and r are the axial and radial coordinates describing the position in the cup. The functions J_0 and J_1 are the zeroth- and first-order Bessel functions of the first kind. A power series expansion exists for $J_0(\mu_j)$. To derive Eq. (24) we have assumed a constant periodic forcing function, $F_0\sin\omega t$. We have also assumed that $I'/I \ll 1$ which is always easy to arrange using this technique.

Equation (24) tells us the fluid motion at all positions in the cup for all frequencies, all viscoelastic parameters, and all sizes and shapes of cup. We can think of it as a superposition of all the normal modes of the fluid motion, thus includes the effects of all modes at every frequency. These equations are valid for all degrees of damping; no small damping approximation was made. Equation (24) has all of the features we expect; the fluid amplitude is the same as that of the cup on the cup boundary, and when $\omega \to 0$. The fluid amplitude away from the boundary vanishes as $\omega \to \infty$. There are fluid resonances at the normal mode frequencies of Eq. (13) in the limit of small damping. The amplitude and Q of these resonances can be found using Eq. (24).

Whereas in the case of the high-Q technique it was necessary to work outside of the double-valued region of Fig. 4, the resonant fluid technique is only useful within that region. Short of a full analysis, it is clear that information can be extracted from resonance curves so long as the Q is somewhat above 1. If both components of the motion A_r and A_i or A and ϕ are measured, then in principle $G(\omega)$ and $\eta(\omega)$ can be calculated over regions of a resonance curve where reasonable data exists. Thus, more information than just G and η on resonance can be calculated. While the data analysis would be somewhat complex, Eq. (24) offers the possibility of extracting much more information regarding the frequency dependence of viscoelastic fluids than previously appreciated.

Using a resonant fluid technique the quality of the data is proportional to the Q. To get data with the same quality as possible with the high-Q technique it is necessary to go to much larger cup sizes, for fixed values of η and G, in order to achieve higher Q's. Since the cup size cannot be practically increased beyond a certain amount the two techniques are essentially nonoverlapping. One technique is always better suited for high-Q data than the other, and should be used for gathering high quality data. Using a high-Q technique, however, a different geometry than the one discussed could always be arranged to get high quality data on the viscoelastic parameters.

IV. VISCOELASTIC MODELS

The fluid whose properties we wish to measure may have an interesting frequency dependence which would be impossible to ascertain by a measurement at only one frequency. To study its frequency dependence using a high-Q technique one would typically construct a sequence of high-Q oscillators over a wide range of frequencies, or use a multiple element oscillator, with more than one useful high-Q resonance. As discussed in Sec. III there exists some potential for extracting $G(\omega)$ and $\eta(\omega)$ over a limited range of frequencies using the resonant fluid technique. In order to expand that range, the cup radius would have to be enlarged, giving more and sharper resonances. In either case, it would be helpful to know the path of $(\lambda/R,\delta/R)$ space traversed by varying the frequency. The answer to this depends, of course, on the frequency dependence of the fluid. There are two simple two-parameter viscoelastic models to consider.[11] Both are extreme simplifications, but their features illustrate some general properties of viscoelastic models, and can be combined to form more complicated models. The following discussion is primarily intended for the high-Q technique, but the considerations of changing resonant frequency in the high-Q technique are analogous to scanning frequency in the resonant fluid technique.

A. Voigt model (viscoelastic solid)

In this model G and η are both independent of frequency and fixed at G_0,η_0. If we fix the cup radius R and vary only the resonant frequency then the measurement will traverse a path where

$$\log_{10}\frac{\lambda}{R} = 2\log_{10}\frac{\delta}{R} + \log_{10}\left[\frac{R(G_0\rho)^{1/2}}{\eta_0}\right] = 2\log_{10}\frac{\delta}{R} - \log_{10}\frac{L}{R}. \quad (25)$$

Lines with varying ω, but constant R are shown in Fig. 7(a). Paths of constant R can be characterized in a dimensionless way by forming the ratio L/R, where $L=\eta_0(G_0\rho)^{-1/2}$. We refer to L as the characteristic "viscoelastic length;" its value only depends on the viscoelastic constants. The value of L/R can be found by noting that $L/R=\delta/R=\lambda/R$ when the line intersects the $\delta/R=\lambda/R$ dividing line, and can be easily read from Fig. 7(a). It is possible to choose a line which traverses the working region shown outlined, but without intersecting the double-valued regions. The longest of these covers a frequency range of about 3 orders of magnitude. It is easy to show that

$$\omega = \frac{G_0}{\eta_0}\left[\frac{\delta/R}{\lambda/R}\right]^2 = \omega_c\left[\frac{\delta/R}{\lambda/R}\right]^2 \quad (26)$$

so that lines of constant ω and varying R are just parallel lines with a slope of 1 as shown in Fig. 7(a). So if we change both ω and R it is possible to traverse paths in the

working region spanning three to four orders of magnitude in frequency. Many of the lines, however, give redundant information regarding the frequency dependence and should be chosen according to the resolution available in that region.

Even though the theoretical possibility exists for measuring G and η, while varying ω and R over a wide range, there are often experimental difficulties associated with doing so. For a fixed R, ω can be decreased by decreasing the torsion constant or by increasing I. When R is varied, so is I'. It is hard to change I' and I by very large amounts but as they are changed it is important to maintain a reasonable ratio of I'/I, for reasons previously outlined. It is clearly best to vary ω by varying the torsion constant within the limits possible.

B. Maxwell model (viscoelastic fluid)

The Maxwell model is a single relaxation frequency model with $\omega_r = G_\infty/\eta_0$, where G_∞ is G as $\omega \to \infty$ and η_0 is η as $\omega \to 0$. It is easily shown that for this model G and η have the form

$$G = \frac{G_\infty}{1+(\omega_r/\omega)^2} \tag{27}$$

and

$$\eta = \frac{\eta_0}{1+(\omega/\omega_r)^2} .$$

If we fix the cup radius R and vary the resonant frequency, the measurement traverses paths as shown in Fig. 7(b). As in the previous case, lines of constant R can most easily be characterized by forming the dimensionless ratio L/R, where $L = \eta_0(2G_\infty\rho)^{-1/2}$. The value of L/R can be read directly from Fig. 7(b) by noting that $L/R = \delta/R = \lambda/R$ at the point where lines of constant R intersect the dividing line $\lambda/R = \delta/R$. Such lines can be described by the equation

$$\log_{10}\frac{\delta}{R} = \tfrac{3}{2}\log_{10}\frac{\lambda}{R} - \tfrac{1}{4}\log_{10}\left[2\left[\frac{L}{R}\right]^2 - \left[\frac{\lambda}{R}\right]^2\right] . \tag{28}$$

When $\omega \ll \omega_r$ the lines have zero slope, when $\omega \gg \omega_r$ the lines have a slope of $\frac{2}{3}$, and $\omega = \omega_r$ when $\lambda/R = \delta/R$. The longest such path traverses 2 orders of magnitude in frequency through the working region. For this case

$$\omega = \omega_r\left[\frac{\lambda/R}{\delta/R}\right]^2 \tag{29}$$

and so lines of constant ω and varying R again are parallel lines of slope equal to 1, as shown in Fig. 7(b). We can see that by choosing R and ω accordingly, data can in principle be taken covering 3 to 4 orders of magnitude in frequency.

It must be emphasized that it is impossible to know what viscoelastic model to apply prior to a measurement without a detailed understanding of the physical system. Real physical systems usually have a complex spectrum of relaxation times. It is hoped that the above treatment gives the reader some feeling for the tradeoffs and constraints involved in designing a cell for the measurement of the frequency dependence of a viscoelastic fluid.

V. CONCLUSION

We have shown that the high-Q oscillating cup viscometer is a very sensitive technique for measuring the viscoelastic parameters G and η of a fluid. This requires the use of an exact expression which we have developed that relates the frequency ω and amplitude α of oscillations to G and η in the well-defined geometry of a right circular cylinder. A method exists for calculating G and η from ω and α which is fast and reasonably convenient. We have derived an exact expression for the fluid motion for all levels of damping, which can be useful for the resonant fluid technique. More information can be extracted concerning the frequency dependence of viscoelastic parameters than has been previously appreciated.

We have shown the region of $(\lambda/R, \delta/R)$ space in which the viscometer is both sensitive and gives unique solutions. This region is surprisingly small, so care must be taken in designing an appropriate oscillator for a particular application. This work suggests the optimal oscillator design to measure a fluid of known viscoelastic parameters. We have also examined the use of the oscillating cup technique for measuring the frequency dependence of the viscoelastic fluid parameters. In principle these can be measured over about four decades of frequency. We have described the tradeoffs involved in designing oscillators to do so in practice. It is hoped that this work will encourage the use of this technique for precise mechanical measurements of viscoelastic fluids.

ACKNOWLEDGMENTS

I would like to acknowledge helpful discussions with D. J. Bishop, G. Agnolet, and R. Pindak.

APPENDIX

For the case of free oscillations Eq. (8) is replaced by the two equations:

$$D_r\left[\frac{\omega}{\omega_0}(-\Delta+i)\right] = -1 + \left[\frac{\omega}{\omega_0}\right]^2 - \left[\frac{\omega\Delta}{\omega_0} - \Delta_0\right]^2 , \tag{A1a}$$

$$D_i\left[\frac{\omega}{\omega_0}(-\Delta+i)\right] = \frac{2\omega}{\omega_0}\left[\frac{\omega\Delta}{\omega_0} - \Delta_0\right] , \tag{A1b}$$

which are a pair of simultaneous transcendental equations for Δ and ω. As for the forced oscillation case these can be solved asymptotically in a few iterations by substituting successive values of Δ and ω back into the expressions for D_r and D_i. This is assisted by solving Eqs. (A1a) and (A1b) for Δ and ω;

$$(\omega/\omega_0) = (1/\sqrt{2})\{(1+D_r)+[(1+D_r)^2+D_i^2]^{1/2}\}^{1/2} , \tag{A2a}$$

$$\Delta = \frac{D_i\omega_0^2}{2\omega^2} + \frac{\Delta_0\omega_0}{\omega} . \tag{A2b}$$

The iteration procedure is started by noting that D_r and D_i are small, so the equivalent of Eq. (9) can be used,

$$\frac{\omega}{\omega_0}=1+\tfrac{1}{2}D_r \ ,$$

$$\Delta=\tfrac{1}{2}D_i+\Delta_0 \ .$$

Evaluation of $D(s)$ becomes more complicated, since the argument $s=(\omega/\omega_0)(-\Delta+i)$ now contains both real and imaginary parts. We will not give the full expression for D_r and D_i for this case, but they can be easily derived from either Eq. (11) or (15) for $D(s)$.

In the absence of fluid, $D_r=D_i=0$ and we see from Eq. (A2) that

$$\omega_e=\omega_0$$

and

$$\Delta_e=\Delta_0$$

by design. The ω_0 and Δ_0 given here are not exactly the same as those given in the text for the forced oscillation case. They differ by terms of order Δ_0^2.

[1]R. N. Kleiman, D. J. Bishop, R. Pindak, and P. Taborek, Phys. Rev. Lett. **53**, 2137 (1984).

[2]E. Dubois-Violette, P. Pieranski, F. Rothen, and L. Strzelecki, J. Phys. (Paris) **41**, 369 (1980); H. M. Lindsay and P. M. Chaikin, J. Chem. Phys. **76**, 3774 (1982).

[3]J. Dubochet, J. Teixera, R. K. Kadiyala, C. M. Alba, D. R. MacFarlane, and C. A. Angell, J. Phys. Chem. **88**, 6727 (1984).

[4]E. G. Shvidkovskii, Uch. Zap. (Moscow University) **74**, 135 (1944); A. M. Butov, L. S. Priss, and E. G. Shvidkovskii, Zh. Tekh. Fiz. **21**, 1319 (1951); L. S. Priss, *ibid.* **21**, 1050 (1952). These three papers have been translated and condensed by J. Kestin and appear in OSR Report No. AF 891/4, 1954 (unpublished).

[5]J. Kestin and G. F. Newell, Z. Angew. Math. Phys. **8**, 433 (1957); D. A. Beckwith and G. F. Newell, *ibid.* **8**, 450 (1957).

[6]J. Kestin and L. N. Persen, OSR Report No. AF 891/2, 1954 (unpublished).

[7]R. N. Kleiman, G. K. Kaminsky, J. D. Reppy, R. Pindak, and D. J. Bishop, Rev. Sci. Instrum. **56**, 2088 (1985).

[8]W. P. Mason, Trans. ASME **69**, 359 (1947). See also K. Sittel, P. E. Rouse, Jr., and E. D. Bailey, J. Appl. Phys. **25**, 1312 (1954).

[9]Tabulation of μ_j's can be avoided by use of the following power series for the μ_j's,

$$\mu_j=\frac{c}{4}\left[1-\frac{6}{c^2}+\frac{6}{c^4}-\frac{4716}{5c^6}+\frac{3\,902\,418}{35c^8}-\frac{8\,952\,167\,292}{35c^{10}}+\cdots\right],$$

where $c=\pi(4j+1)$.

[10]While it seems that the resolution should also improve with increasing Q, the assumption of a fixed noise level independent of the Q is a good one as long as the Q is reasonably high because the noise level becomes limited by other factors. Thus an enhancement of the Q will not give rise to a further improvement in the noise level.

[11]J. D. Ferry, *Viscoelastic Properties of Polymers* (Wiley, New York, 1980).

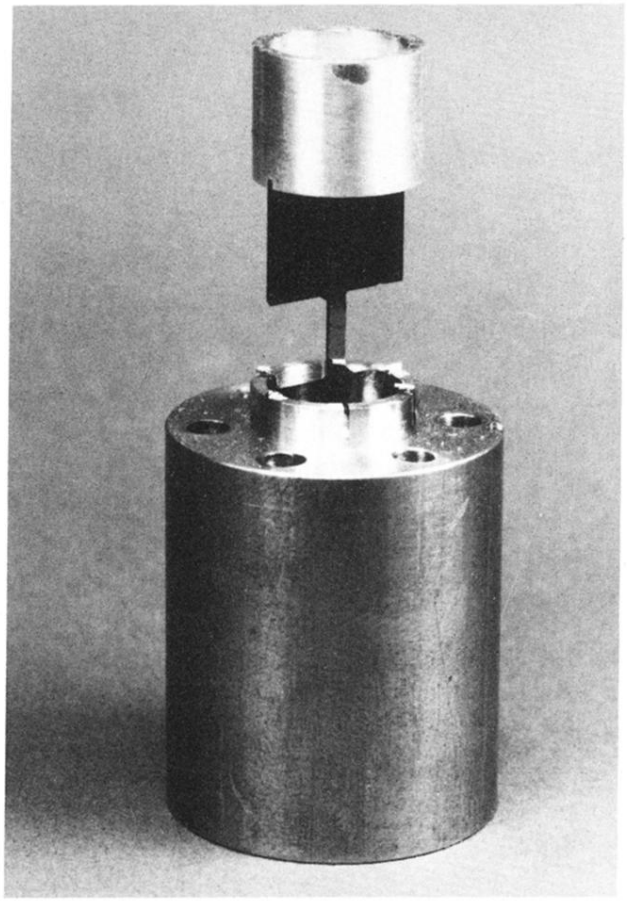

FIG. 1. High-Q torsional oscillator configured as an oscillating cup viscometer. Viscoelastic parameters of a sample can be deduced by measuring the resonant frequency and amplitude of the oscillator when empty and in the presence of the sample. For this oscillator $Q_0 \approx 10\,000$ and $\omega_0 = 128$ Hz.